EINDHOVEN UNIVERSITY OF TECHNOLOGY

Novel wafer-scale adhesive bonding with improved alignment accuracy and bond uniformity

Citation for published version (APA):
Abdi, S., de Vries, T., Spiegelberg, M., Williams, K. A., & Jiao, Y. (2023). Novel wafer-scale adhesive bonding with improved alignment accuracy and bond uniformity. *Microelectronic Engineering*, *270*, Article 111936. https://doi.org/10.1016/j.mee.2023.111936

Document license:
CC BY-NC-ND

DOI:
10.1016/j.mee.2023.111936

Document status and date:
Published: 01/02/2023

Document Version:
Publisher's PDF, also known as Version of Record (includes final page, issue and volume numbers)

Please check the document version of this publication:

• A submitted manuscript is the version of the article upon submission and before peer-review. There can be important differences between the submitted version and the official published version of record. People interested in the research are advised to contact the author for the final version of the publication, or visit the DOI to the publisher's website.
• The final author version and the galley proof are versions of the publication after peer review.
• The final published version features the final layout of the paper including the volume, issue and page numbers.

Link to publication

General rights
Copyright and moral rights for the publications made accessible in the public portal are retained by the authors and/or other copyright owners and it is a condition of accessing publications that users recognise and abide by the legal requirements associated with these rights.

• Users may download and print one copy of any publication from the public portal for the purpose of private study or research.
• You may not further distribute the material or use it for any profit-making activity or commercial gain
• You may freely distribute the URL identifying the publication in the public portal.

If the publication is distributed under the terms of Article 25fa of the Dutch Copyright Act, indicated by the "Taverne" license above, please follow below link for the End User Agreement:

www.tue.nl/taverne

Take down policy
If you believe that this document breaches copyright please contact us at:

openaccess@tue.nl

providing details and we will investigate your claim.

Download date: 17. Nov. 2023

Microelectronic Engineering 270 (2023) 111936

Contents lists available at ScienceDirect

Microelectronic Engineering

journal homepage: www.elsevier.com/locate/mee

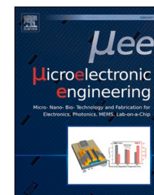

Novel wafer-scale adhesive bonding with improved alignment accuracy and bond uniformity

Salim Abdi [a,*], Tjibbe de Vries [b], Marc Spiegelberg [a], Kevin Williams [a], Yuqing Jiao [a]

[a] Eindhoven Hendrik Casimir Institute (EHCI), Eindhoven University of Technology, Eindhoven 5600MB, the Netherlands
[b] Nanolab@TU/e, Eindhoven University of Technology, Eindhoven 5600MB, the Netherlands

A R T I C L E I N F O

Keywords:
3D integration
Heterogeneous integration
Adhesive bonding
Alignment accuracy
Process uniformity

A B S T R A C T

We report a versatile method for improving post-bonding wafer alignment accuracy and BCB thickness uniformity in stacks bonded with soft-baked BCB. It is based on novel BCB-based micro-pillars that act as anchors during bonding. The anchor structures become a natural part of the bonding interface therefore causing minimal interference to the optical, electrical and mechanical properties of the bonded stack. We studied these properties for fixed anchor density and various anchor heights with respect to the adhesive BCB thickness. We demonstrated that the alignment accuracy can be improved by approximately an order of magnitude and approach the fundamental pre-bond alignment accuracy by the tool. We also demonstrated that this technique is effective for a large range of BCB thicknesses of 2–16 μm. Furthermore we observed that the thickness non-uniformities were reduced by a factor of 2–3 × for BCB thicknesses in the 8–16 μm range.

1. Introduction

Wafer-scale bonding using adhesive polymers is a crucial processing step for multiple state-of-the-art microelectromechanical (MEMS) devices [1], photonic integrated circuits (PICs) [2,3], and in device packaging applications [4]. For photonics, adhesive bonding enabled heterogeneous integration of novel nano-photonic platforms offering high integration density, low energy consumption, and monolithic vertical co-integration with electronic devices [2,3,5].

The polymers used in this method, such as Benzocyclobutene (BCB), are compatible with most of the standard fabrication flows in terms of the thermal budget, material choice, and post-bonding processing. But to ensure a void-free bond with high post-bond mechanical strength and high tolerance to surface topography, low cross-linked (soft-baked) BCB is required [4,6]. This is because the latter achieves low viscosity during bonding, hence wetting the bonding interfaces [4,7]. BCB with higher cross-linking percentages turns into a gel-like state with no adaptability to surface topography. Thus, the bond can suffer from significant void formation and unbonded areas [7,8]. However, bonding with soft-baked BCB results in degraded post-bonding alignment accuracy and BCB thickness uniformity. Moreover, the thickness of soft-baked BCB is required to be around 1.5–2 times the height of topographies in the two interfaces to result in void-free bonding, but higher thicknesses lead to larger degradation of these parameters [6].

High alignment accuracy is crucial for bonding applications where functional devices are vertically stacked, including vertical co-integration of photonics with electronics [3]. With state-of-the-art bonding tools, the attainable pre-bond accuracy is below 3 μm [9]. However, The post-bonding alignment accuracy with soft-baked BCB degrades quickly up to an order of magnitude higher [6,7,9]. This is caused by the unavoidable presence of shear forces during bonding, acting significantly during the low viscosity state of BCB sandwiching the two substrates.

There are multiple ways to tackle post-bonding misalignment for soft-baked BCB. Using partially-cured BCB allows for better alignment accuracy but with no benefits of BCB reflow [8], leading to void formation for structured bonding interfaces [6]. Accounting for misalignment in the design layout results in larger devices and lowers the integration density and/or optimal device performance. Further, Song *et al* [7] proposed to calculate the shift in misalignment using front-runners, and pre-compensating for it in the real identical wafers. But this requires running double experiments if any processing condition is changed, and the method is not reliable for all material systems [6,9]. Hence, processes that directly block misalignment are preferred. For instance, mechanical anchors can be fabricated to join the two wafers together during bonding and hence limit misalignment [4]. Al-based

* Corresponding author.
E-mail address: s.a.abdi@tue.nl (S. Abdi).

https://doi.org/10.1016/j.mee.2023.111936
Received 17 November 2022; Received in revised form 4 January 2023; Accepted 7 January 2023
Available online 10 January 2023
0167-9317/© 2023 The Author(s). Published by Elsevier B.V. This is an open access article under the CC BY-NC-ND license (http://creativecommons.org/licenses/by-nc-nd/4.0/).

anchors were tested for 2-μm thick BCB and provided good anchorage with lower misalignment [9]. Interlocking anchors were also investigated for various systems, and 0.2-μm thick BCB [10,11]. However, asides from the bond-quality issues, both methods were only tested for <1 μm-thick BCB. They are also difficult to be integrated in mature process flows because of the complex fabrication and possible incompatibilities with standard flows. For instance, compatibility checks are needed before depositing and patterning thick metals or semiconductors for anchors on semi-processed wafers. Moreover, using interlocking anchors for bonding substrates of different coefficient of thermal expansion (CTE) is not possible, as the latter would expand and retract at a different rate during bonding. These methods also increase dead space where no device or fabrication test structures can be placed.

Another compromise of soft-baked BCB is the significant post-bonding thickness non-uniformity [12]. Good thickness uniformity after bonding is important in multiple aspects. First, if post-bonding processing requires etching of the adhesive film to fabricate through-polymer interconnections for instance, it becomes complicated to open all areas. Secondly, thickness variations can directly affect device performance. Moreover, for IMOS active devices [5], the heat is mainly dissipated through the Si carrier wafer. Higher thicknesses yield lower heat dissipation and therefore degraded performance [6]. Moreover, for grating couplers, variations in the bonding thickness yield variation in the coupling efficiency depending on the interference [13]. Therefore, high thickness non-uniformities lead to unpredictable and possibly degraded device performance. To our knowledge, there are no current methods that tackle this issue for bonding with soft-baked BCB.

In this paper, we investigated the possibility to use wafer-scale uniformly-distributed BCB-based anchors to improve the post-bonding alignment accuracy and BCB thickness uniformity. The BCB anchors are fully crosslinked, serving as solid anchor structures. Unlike other anchor methods, the proposed method offers minimal change to the optical, electrical and mechanical properties of the bonding interface, because the anchors and the bonding layer are based on the same material. As a result, the method achieves a uniform bonding layer and does not increase dead space nor influence post-bonding processing. It can also be applied to other polymers used in adhesive bonding if the anchors are dense and have sufficient mechanical strength to serve their intended purpose. Here, we fixed the density of anchors (fill ratio) at 20% and systematically studied the effect of adding the anchors to the bonding process for BCB thicknesses in the 2–16 μm range. The physical characteristics of anchors and important parameters for post-bonding processing were also investigated.

2. Experimental details

In this study, we chose to bond identical wafers, *i.e.* no CTE mismatch to avoid having post-bonding geometric distortions and misalignment due to expansion, hence limiting misalignment to substrate shifts alone [10,14]. Moreover, given that misalignments from expansion need to be corrected in the mask layout in any case, this method can be applied to heterogeneous substrates as well. Therefore, we used glass-glass wafers with markers to study the alignment accuracy, as their transparency helps in verifying the pre-bond alignment and facilitates characterization. We also used bare InP-InP wafers to study the thickness uniformity, since reflectometry was used for accurate thickness mapping after removing the top wafer. Details of all experiments are listed in the results section (Table 1 and 2). The general process flow we followed to fabricate the wafers and bond them is shown in Fig. 1.a). An illustration of the pre- and post-bonding wafer stacks are shown in Fig. 1.b) and .c), respectively.

For the glass wafers, we used 3″ double-side polished Fused Silica Wafers with a bow of <20 μm and thickness of 500 μm. For the InP wafers, we used test-grade wafers with bows of <30 μm and thickness of 650 μm. The bows of each wafer were measured using profilometry and matched such that wafer 1 and 2 (Fig. 1) have a similar bow profile and values. The latter is realized to avoid having high bow mismatch that can potentially introduce post-bonding residual stresses and thickness variations, which can introduce additional errors in our results [15]. As a result, the bow of the bonded stack was also minimized.

We start the fabrication by pre-cleaning the substrates in O2 plasma. Next for the glass wafers, we deposit and pattern 10/100 nm-thick Ti/Au alignment markers *via* lift-off. The pattern consists of 12 alignment keys distributed along 2 rows in the wafer. Subsequently, we deposit and outgas 500-nm thick SiO2 layer, and spin-coat monolayer of AP3000 to optimize the adhesion of BCB to the wafers.

We studied BCB thicknesses of 2, 4, 8, and 16 μm, so we used Cyclotene 3022–46, −57, and − 63 at different RPMs to achieve these target thicknesses with optimal uniformity after spin-coating. For wafer 2 (Fig. 1a), the BCB is then soft-baked at 100 °C for 5 min, and an extra layer of AP3000 is applied to improve adhesion of BCB to the BCB anchors during bonding. To fabricate anchors on wafer 1, we used the same BCB in wafer 2 to investigate the variation in physical properties between the two. After BCB deposition and soft-bake, we hard-bake the stack in N2 environment at 280 °C for 1 h to ensure full-crosslinking of BCB inside anchors. Next, we spin-coat 25-μm thick AZ9260 and pattern it *via* photolithography, then we subsequently transfer the pattern to BCB with O_2:CHF_3 20:4 plasma RIE etching and reapply a final layer of AP3000. It is important to note that a 12% reduction in height is obtained after hard-baking BCB, therefore, the anchors in wafer#2 are 12% shorter than soft-baked BCB in wafer#1 before bonding.

To bond the wafers, we first align them in commercial EVG aligner using the crosshair method, whereby the markers of wafer 2 are located and crosshairs of these markers is registered in the system, then markers of wafer 1 are aligned to those crosshairs. Next, the wafers are brought into contact and we visually inspect the alignment, then lock the stack in

Table 1
Wafer-scale misalignment of all glass-glass bonding experiments.

Experiment number	BCB thickness (μm)	Anchors thickness (μm)	average shift in x-direction (μm)	average shift in y-direction (μm)	total misalignment (μm)
1	2	0	4.6	29.5	29.9
2	2	0	1.0	32.6	32.6
3	2	2	2.8	1.7	3.3
4	2	2	1.2	0.5	1.3
5	8	0	36.5	1.5	36.5
6	8	0	58.0	12.0	59.2
7	8	0	13.0	8.0	15.3
8	8	4	1.6	15.6	15.7
9	8	4	6.6	6.1	9.0
10	8	8	6.2	4.6	7.7
11	8	8	3.2	2.2	3.9
12	16	0	137.0	47.0	144.8
13	16	0	40.0	18.0	43.9
14	16	16	7.8	1.1	7.9
15	16	16	3.0	2.0	3.6

Table 2
BCB post-bonding thickness variations obtained from reflectometry. Exp N.16 represents a Hard-baked BCB reference without bonding. Exp N.17 represents a reference stack bonded using partially baked BCB at 175 °C for 1 h.

Experiment number	BCB thickness (μm)	BCB anchors height (μm)	Lowest thickness (nm)	Highest thickness (nm)	Average thickness (nm)	Normalized Variation (%)	Standard Deviation (nm)
16	8	0	8499	8615	8545	1.4	28
17	8	0	7786	8562	8050	9.6	150
18	8	0	4431	10971	7219	90.6	2411
19	8	0	3833	11096	8510	85.3	1604
20	8	0	712	10079	7644	122.5	1938
21	8	8	7736	9545	8514	21.2	528
22	8	8	6999	10161	8508	37.2	973
23	8	8	7079	11009	8510	46.2	979
24	16	0	3271	20216	14463	117.2	3841
25	16	0	7961	18162	13574	75.2	2938
26	16	16	15483	22523	17671	39.8	1482

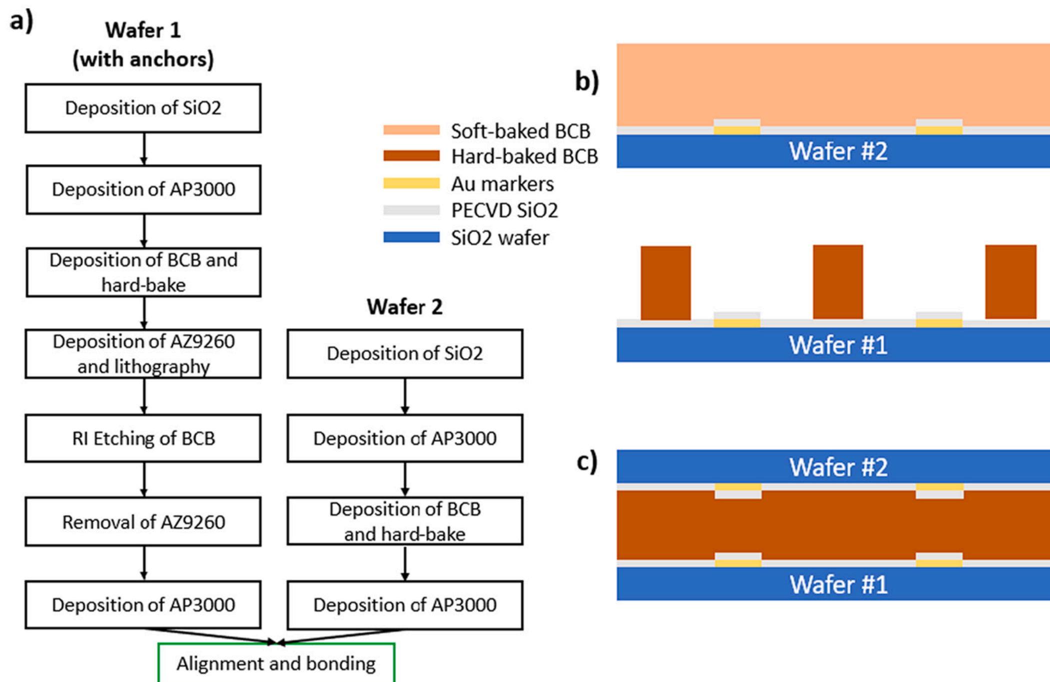

Fig. 1. a). Fabrication process flow of the full bonding stack. Illustration of the bonding stack using BCB anchors: b). Pre-bonding, c). Post-bonding.

a cassette holder. This procedure allows us to achieve 1–2 μm accuracy. The cassette is then loaded into EVG bonder. Bonding is realized in vacuum ($<10^{-5}$ Torr) where the stack is heated at a rate of 5 °C/min while applying a force of 700 N, the force is then released and a full-cure of 1 h at 280 °C is realized.

For the InP stacks after bonding, wafer 2 is selectively etched in HCl: H2O 4:1 at 35 °C to reveal the adhesive layer. Evidently, a dielectric multi-layer is deposited on the backside of wafer 1 before etching to protect it.

This seamless fabrication of anchors means that they can be put anywhere in the wafer. Therefore for the mask layout, we chose a real layout used in the co-integration of PICs with electronics. The mask layout consists of different (5 × 5) mm reticles that are repeated throughout the wafer. The average size of these rectangular anchors inside each reticle is around 0.1 × 0.1 mm^2 and the minimum spacing between anchors is ≈10 μm. Also, given that shear forces present during bonding are low compared to compression forces [7], a fill factor (density of anchors relative to empty space) of ≈1% was enough to block misalignment using Al-based anchors [9]. In our case, the hardness of BCB is ≈20× lower than Al sputtered thin films [16,17], and considering that these anchors do not increase dead space, we fixed the density to 20% for all of our experiments using BCB anchors.

After fabrication, all stacks are inspected using optical microscopy to calculate the misalignment and assess void formation, SEM to inspect the interface between BCB and BCB anchors, and reflectometry with profilometry for thickness measurements. We also used NIR ellipsometry to extract the optical properties of BCB. For that, we fitted the results using the Cauchy model with MSE <50. For reflectometry, each map was obtained with 65 points evenly distributed across the 3"wafer, and we used 3 mm edge exclusion in all maps.

3. Results and discussions

3.1. Misalignment

For BCB bonding of wafers with identical CTE, misalignment errors mainly result from shifts (translations) in the (x,y) plane. Rotations are minimized in state-of-the-art tools, and orthogonal and non-orthogonal expansions only result from CTE mismatch between the bonded wafers [12]. The designed role of anchors is to provide solid mechanical support between the two wafers during bonding, and thereby limit the misalignment. Therefore, misalignment due to rotation might also be

suppressed using this method, if present.

Results on the wafer-scale shifts of all experiments are listed in Table .1. Here, we considered the average shift of all 12 alignment keys since the variation between individual values is small given the identical CTE between wafers and negligeable post-bonding rotation. Moreover, the anchors are supposed to block shifts regardless of the direction, which is why we simplify our analysis by using the total misalignment. Results are plotted in Fig. 2.a for stacks without *vs* with anchors having matching heights to the bonding thickness. We also included the average values of alignment keys from [18] given that similar bonding parameters with soft-baked BCB were used. For Fig. 2.b, we plot misalignment *vs* height ratio of anchors for matrix BCB thickness of 8 μm.

Starting with bonded stacks without anchors, the wafer-scale total misalignment increases significantly with increasing BCB thickness (Fig. 2.a), This is because soft-baked BCB reflows during the bonding, and thereby serves as a lubricant with higher viscoelasticity for higher thicknesses, allowing one wafer to shift from the original position with respect to the other [4]. This wafer-scale shift is attributed to the presence of shear forces during the reflow state of BCB [7]. We also note that the shift values in x-direction are higher than in the y-direction for 8- and 16-μm BCB, and *vice versa* for 2-μm BCB, which signifies an interplay between a preferred directionality (systematic shift) and non-directionality that are affected by BCB thickness.

In our bonding process, this systematic shift is likely caused by an uneven clamping force of the cassette holder, since the clamping force was intentionally lowered to avoid cracking of the fragile InP wafers, and the x-direction is on the same axis of the two pins in the holder. It is worthwhile to note that these EVG bonder and bond aligner imperfections fall within its fabrication tolerances and cannot be improved. A consistent wafer-scale systematic shift was expected for similar bonding conditions depending on the value of shear forces and viscosity of BCB [7]. However, high variance was recorded in our results and also from Niklaus [8,9]. This variance is attributed to inhomogeneities in the BCB reflow process during the bonding caused by non-uniform compression [18]. Indeed, the thickness variation stays high as the BCB thickness increases (as discussed in the Sec.II.2), and the absolute thickness variations also further diverges for higher BCB thicknesses leading to high variance. Moreover, wafer bow and shear force non-uniformities caused by the total thickness variation (TTV) of the wafers might also contribute to this variance [7,15]. This variance might also be exacerbated by the presence of particles at the bonding interface, since particles with larger dimensions than the bonding thickness, which would force the reflow of BCB to accommodate its presence depending on the compression force it can handle. Therefore, uneven distribution and concentration of sandwiched particles can contribute to variations in the random shift between samples. However, the effect of particles presence does not explain the increase in variance when the thickness increases. Investigating the variance itself is indeed cumbersome as it would require repeating the experiment multiple times to gather enough data for mapping the edges of the variance, which is outside the scope of this paper.

For the bonded stacks having anchors with the same height as the matrix (Fig. 2.a), The wafer-scale shifts after bonding are lower than 10 μm for 8- and 16-μm BCB and $<$ 5 μm for 2-μm BCB. These results are comparable to anchors fabricated with Aluminum along the edge of the wafer [9]. In both cases, the presence of anchors between the two wafers suppresses the shift to a good extent. Moreover, both systematic and non-systematic shifts are suppressed to a good extent (Table .1) whereas the variance in misalignment between samples is also comparably high, signifying that the anchors do not fully suppress one mechanism above the other. Moreover, the variance does not significantly increase when the thickness is varied from 2 to 16 μm highlighting that the anchorage works in a similar manner for all thicknesses.

As will be discussed in Sec II.2 on the thickness variation suppression using anchors, the existence of thickness variation with samples having anchors can be the reason for the incomplete suppression of the shift with the anchors. This is because regions with low pressure during bonding would have a higher thickness than the intended thickness, and thereby anchors in these regions do not reach the other substrate, hence reducing the effective density of working anchors. To investigate this, we varied the height of anchors relative to a matrix thickness fixed at 8 μm. Results are shown in Fig. 2.b. Indeed, we see that both misalignment and variance in misalignment increases for bonding experiments with anchors having a height ratio of 0.5 compared to 1.

Finally, the introduced BCB-based anchors added frictional forces between the two substrate surfaces that acted against the shear forces during the liquid state of BCB, resulting in lower misalignment. This mechanism can therefore be extended to inhibit wafer shifts being the main or a component of the total misalignment in other systems that involve BCB bonding, such as bonding InP to InP or InP to Si.

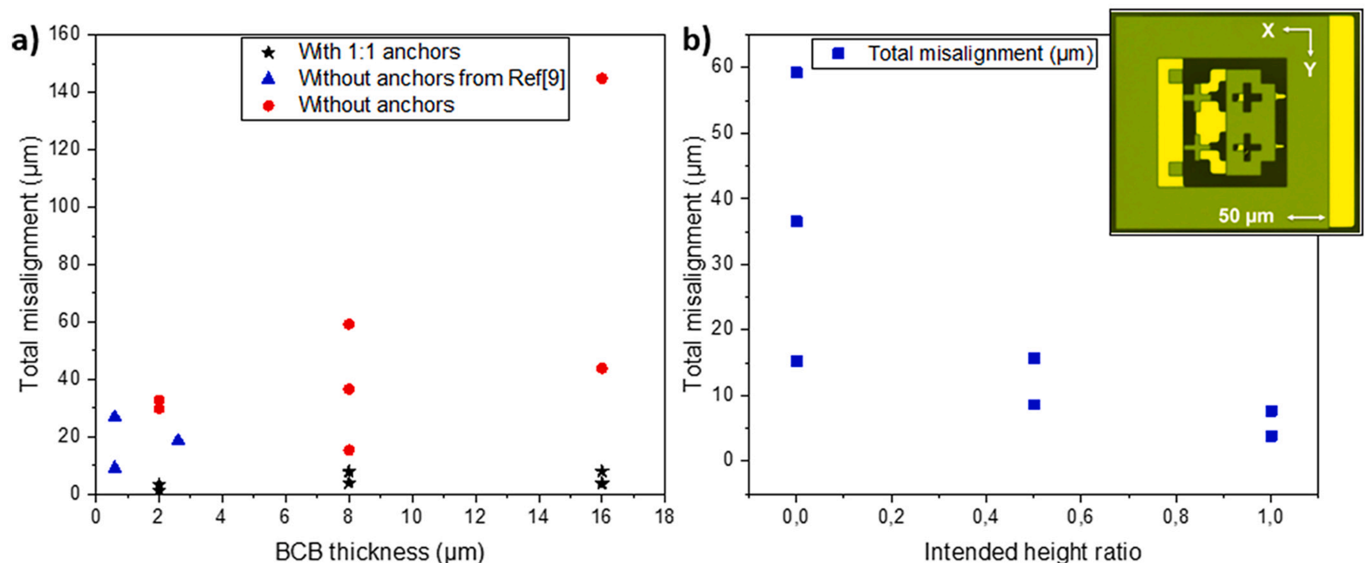

Fig. 2. a). Total misalignment of bonded glass stacks with and without 1:1 height ratio anchors *vs* BCB thickness. b). Total misalignment of bonded glass stacks with 8 μm BCB matrix *vs* anchors height ratio. Inset: microscope image of misaligned markers N5.

3.2. Thickness uniformity

An image of the BCB fringe pattern and reflectometry map of samples from Exp N.20 and N.22 are shown in Fig. 3. The reflectometry maps are analyzed and results are summarized in Table.2. Asides from experiments on soft-baked BCB, we also fabricated and analyzed 2 reference samples. In Exp N.16 we measure a fully cured BCB after spin-coating, and in Exp N.17 we used 8-μm thick BCB layer that was partially cured at 175 °C for 1 h to bond InP-InP stack with the same bonding parameters as before. The goal was to assess the thickness non-uniformity for bonding using partially-cured BCB, which we expect to be better than soft-baked BCB [8].

As seen in Fig. 3.a) compared to 3.c), the wafer-scale BCB fringes are denser, which signify higher thickness variations when anchors are not employed. Moreover, the min and max locations are randomly distributed along the wafer without preferred location in most of the samples. This might be related to the presence of randomly placed particles with higher dimensions that force redistribution of the liquid BCB, or non-uniform presence of residual forces, for instance during clamping of the cassette while alignment or because of TTV of the wafers.

Looking at results from Table .2. The thickness variation for the hard-baked BCB reference is only 1.3% since high uniformity is expected after spin-coating. This uniformity also translates to high uniformity in the thickness of anchors used for subsequent bonding. The thickness variation in the partially-cured reference is 9.6% however. This is because the bonded area in this experiment is ≈ 80% of the total wafer thickness, due to the existence of a BCB edge bead of 15-μm that inhibits bonding the full area without applying high force. The thickness variation range of samples without anchors is ≈90–120% and ≈75–120%, for 8- and 16-μm BCB, respectively. This is caused by the reflow of BCB during bonding, which allows it to be expelled from high compression points and accumulate near low compression regions in the wafer. The source of this variation might be attributed to multiple reasons, like using test-grade wafers having small defects, different matched bows, residual stresses after clamping the wafers… However, the goal here was to demonstrate the trend in improvement using BCB anchors and not optimize the uniformity.

The range is reduced to ≈21–46% and 40% for 8 and 16 μm samples, respectively for samples with anchors matching the height of the BCB thickness. Moreover, because of local thickness variations, some regions have a higher thickness compared to the intended thickness, and hence a lower percentage of anchors reaches the other substrate. Although it is difficult to pinpoint the exact value for this *effective* density, the designed density of 20% was sufficient in reducing the thickness non-uniformities.

Moreover, the average BCB thickness for samples without anchors is higher than that with anchors for both 8 and 16 μm samples. We suspect that the volume occupied by anchors (20%) is not fully dissipated from the matrix during the short time when BCB is liquid such that the measured average post-bonding thickness is the same as the intended value. This could be due to the lower bonding pressure applied to avoid breaking wafers. Hence we note that the fill ratio of anchors needs to be accounted for in choosing a lower corresponding thickness of matrix BCB for optimal anchoring. The correct thickness might depend on multiple parameters such as the fill factor of anchors, applied bonding force, ramp-up speed …*etc.*

Given the randomness of max and min points (Fig. 3.b and d), an optimal performance of anchors can be achieved with a uniform distribution of anchors along the wafer rather than having anchor concentrated only in specific locations, for ex: the wafer edges [9]. This ensures that the anchors block redistribution of BCB from high to low compression points.

Finally, The introduced anchors' hardness and their uniform wafer-scale distribution provided mechanical support to suppress non-uniformities in the applied bonding force. This consequently resulted in lower redistribution of BCB during its liquid state to accommodate for

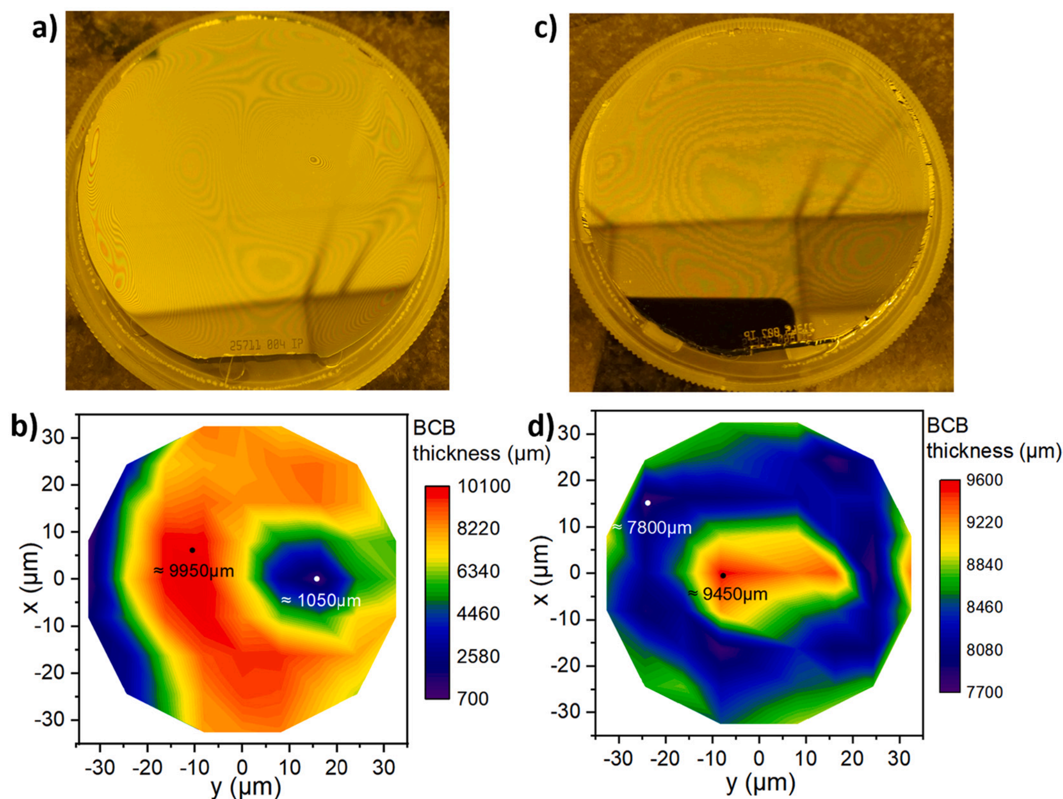

Fig. 3. a). BCB pattern of a bonded stack without anchors Exp 20, and b). its corresponding reflectometry map. c) BCB pattern of a bonded stack with 1:1 anchors Exp 22, and d). its corresponding reflectometry map.

these forces, and hence lower non-uniformities. This method is therefore applicable to other systems regardless of the source of variations in the compression forces. If these parameters are controlled, a higher/lower density of anchors can be used for higher/lower variations in the compression force.

3.3. Physical properties

Fig. 4.a) shows an SEM picture of anchors before bonding and Fig. 4b) shows a cross-sectional picture of the anchors after bonding near the anchor-BCB interface. It can be seen that the interface is perfectly continuous without introduction of voids, The dark line at the interface is apparent because of electric charging during the long exposure to acquire the image. Here, BCB reflows well to cover the areas between anchors without leaving voids (See Fig. 5).

Moreover, we uniformly RIE etched 2-μm deep into BCB to reveal the interface between the anchors and matrix, an angled top-view SEM image of this interface is shown in Fig. 4.c). Here, the interface between anchors and the matrix (highlighted in red) is not interrupted by any void. The surface pattern inside anchors is denser compared to the matrix, which is related to the different thermal treatment history of BCB inside anchors and the matrix. This is believed to be caused by the vitrification of BCB whereby the free volume of BCB is decreased, and hence a denser pattern is obtained [19].

Furthermore, we assessed the optical properties of anchors relative to the matrix to determine if the anchors can be placed near photonic devices. For this NIR ellipsometry measurements were carried out on reference samples. The samples consisted of 1-μm thick BCB treated at 280 °C for 1 h and 2 h, and at 250 °C for 1 h and 2 h. The latter was additionally investigated given that full curing can be achieved at that thermal budget [18]. We chose this thickness to obtain the highest fit possible given that our interest lies in the refractive index difference.

The measured refractive index difference for samples treated at 250 °C is below 0.025 over the full wavelength range, whereas the variation for samples treated at 280 °C decreases steeply from 0.08 at 300 nm to 0.025 at 600 nm and stabilizes below this value at higher wavelengths. This is largely because of the higher shrinkage of BCB when cured at a higher thermal budget (time and temperature) [8,19]. The fitted thicknesses are 1080 ± 2.5 and 1073 ± 2.5, 1047 ± 3 and 994 ± 3 for samples treated at 250 for 1 and 2 h, and 280 for 1 and 2 h, respectively. So the difference in thickness is 7 ± 5 nm and 53 ± 6 nm for samples treated at 250 and 280 respectively, which support the higher condensation for higher thermal budgets.

One crucial post-bonding processing step for co-integration of photonics with electronics is BCB etching [3]. We used the reference samples previously discussed to determine the etch rate difference between samples treated at a higher thermal budget. We found that the etch rate difference is below 3% for samples treated at 250 and 5% for samples treated at 280 (Fig. 4.c). This slight variation in etch rates is related to the higher density of BCB treated at higher thermal budgets [19]. Therefore, no optimizations of post-processing steps are required and the design of anchors in terms of shape and distribution is not constrained.

For further improvements to achieve anchors with matching optical properties to the matrix, optimizing the thermal budget to maintain good mechanical properties of anchors and close physical properties relative to the matrix might be an option. By good mechanical properties we refer to high hardness and young's modulus for the anchors so that they sustain higher compression pressure without plastically deforming. For the choice of thermal budget for anchors, other factors can also be included in this choice such as higher adhesion between anchors and the matrix. In fact, instead of ≈100% crosslinking, it could be better to choose lower cross-linking percentages to better match the thermal budget with the matrix BCB. For BCB, the optimal crosslinking percentage of anchors is at 85–90% instead of 100%. This can lead to an improvement in adhesion to matrix BCB by a factor of 3-4× [20] while the Hardness stays relatively the same and young modulus only reduces by ≈1.2–1.5× [16]. Finally, we demonstrated improved post-bonding alignment accuracy and bond uniformity with a fixed anchor fill factor of 20%. The fill factor can be further investigated to find the boundaries of this method.

4. Conclusions

In this work, we used BCB-based anchors to improve the post-bonding thickness uniformity and alignment accuracy for a wide range of BCB thicknesses. By using BCB anchors, the alignment accuracy improved by an order of magnitude to approach the fundamental pre-bond alignment accuracy of the tool for BCB thicknesses in the 2–16 μm range. And the thickness uniformity improved by a factor of 2-3× for BCB thicknesses in the 8–16 μm range. We also highlighted the importance of matching the height of anchors to the BCB thickness used for bonding for better alignment accuracy. Finally, an added advantage to using the same BCB for anchors and adhesive bonding is the similar physical properties between the two after bonding and seamless fabrication of anchors.

Funding

This work was supported by the H2020 ICT TWILIGHT Project (contract No. 781471) under the Photonics PPP.

Disclosures

The authors declare no conflicts of interest.

Credit author statement

Salim ABDI: Writing - original draft, Conceptualization, Methodology, Investigation, Visualization.

Tjibbe de Vries: Conceptualization, Methodology.

Marc Spiegelberg: Validation.

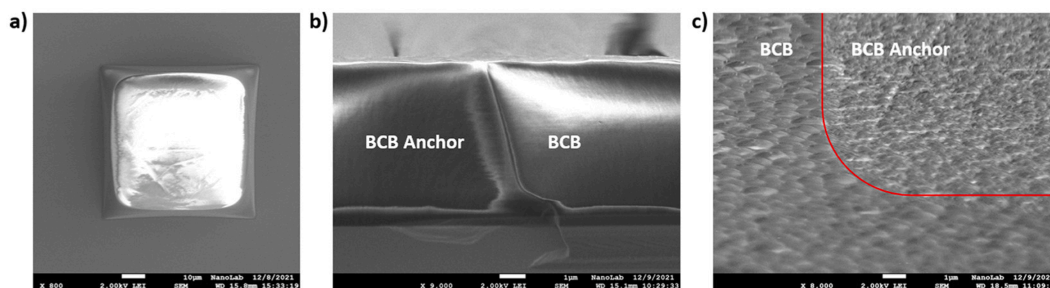

Fig. 4. a). Top view of a standalone BCB anchor before bonding. Post-bonding interface between 8-μm BCB and 8-μm BCB anchors (Exp N:21: b). cross-sectional view c). Angled top-view after uniformly etching 2-μm deep into BCB.

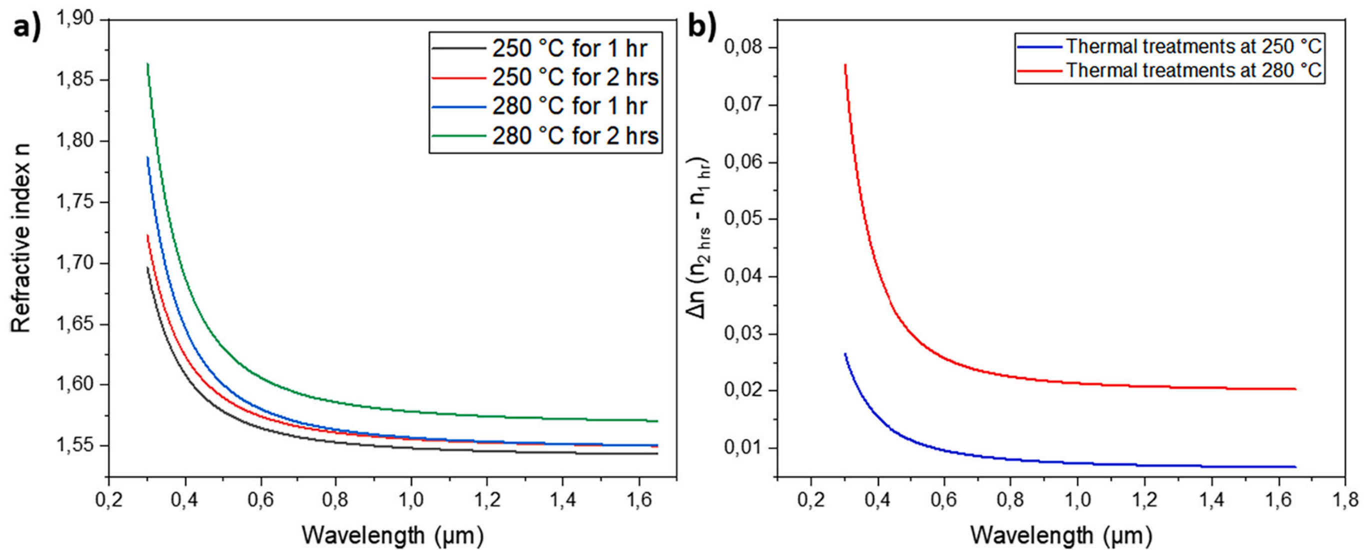

Fig. 5. a) Refractive index of BCB treated at different conditions. b) Refractive index difference for BCB treated at different times and fixed temperature.

Kevin Williams: Supervision, Funding acquisition.

Yuqing Jiao: Supervision, Writing - review & editing, Funding acquisition.

Declaration of Competing Interest

The authors declare the following financial interests/personal relationships which may be considered as potential competing interests:

Yuqing Jiao reports financial support was provided by the H2020 ICT TWILIGHT Project (contract No. 781471) under the Photonics PPP. Salim has patent "A method for bonding a first and second planar substrate" pending to Dutch provisional patent No. 2032112.

Data availability

Data will be made available on request.

Acknowledgments

The research was performed in the NanoLab@TU/e cleanroom facility. The authors acknowledge Cristian A.A.van Helvoirt from Department of Applied Physics at TU/e for his ellipsometry measurements.

References

[1] M. Lapisa, G. Stemme, F. Niklaus, Wafer-Level Heterogeneous Integration for MOEMS, MEMS, and NEMS, IEEE J. Sel. Top. Quantum Electron. 17 (2011) 629–644.
[2] Y. Jiao, N. Nishiyama, J. van der Tol, J. van Engelen, V. Pogoretskiy, S. Reniers, A. A. Kashi, Y. Wang, V.D. Calzadilla, M. Spiegelberg, Z. Cao, K. Williams, T. Amemiya, S. Arai, InP membrane integrated photonics research, Semicond. Sci. Technol. 36 (2020), 013001.
[3] W. Yao, X. Liu, M.K. Matters-Kammerer, A. Meighan, M. Spiegelberg, M. Trajkovic, J.J.G.M. van der Tol, M.J. Wale, X. Zhang, K. Williams, Towards the Integration of InP Photonics With Silicon Electronics: Design and Technology Challenges, J. Lightwave Technol. 39 (2021) 999–1009.
[4] X. Wang, F. Niklaus, "Polymer Bonding," in 3D and Circuit Integration of MEMS, John Wiley & Sons, Ltd, 2021, pp. 331–359.
[5] F. Niklaus, G. Stemme, J.-Q. Lu, R.J. Gutmann, Adhesive wafer bonding, J. Appl. Phys. 99 (2006), 031101.
[6] Y. Jiao, J. van der Tol, V. Pogoretskii, J. van Engelen, A.A. Kashi, S. Reniers, Y. Wang, X. Zhao, W. Yao, T. Liu, F. Pagliano, A. Fiore, X. Zhang, Z. Cao, R. R. Kumar, H.K. Tsang, R. van Veldhoven, T. de Vries, E.-J. Geluk, J. Bolk, H. Ambrosius, M. Smit, K. Williams, Indium Phosphide Membrane Nanophotonic Integrated Circuits on Silicon, Phys. Status Solidi A 217 (2020) 1900606.
[7] M. Spiegelberg Tol, J.J.G. M., K.A. Williams, 3D-Integration on Wafer Level of Photonic and Electronic Circuits, Technische Universiteit Eindhoven (2021).
[8] Z. Song, Z. Tan, L. Liu, Z. Wang, Void-free BCB adhesive wafer bonding with high alignment accuracy, Microsyst. Technol. 21 (2015) 1633–1641.
[9] F. Niklaus, R.J. Kumar, J.J. McMahon, J. Yu, J.-Q. Lu, T.S. Cale, R.J. Gutmann, Adhesive Wafer Bonding Using Partially Cured Benzocyclobutene for Three-Dimensional Integration, J. Electrochem. Soc. 153 (2006) G291.
[10] F. Niklaus, P. Enoksson, E. Kälvesten, G. Stemme, A method to maintain wafer alignment precision during adhesive wafer bonding, Sensors Actuators A Phys. 107 (2003) 273–278.
[11] S.H. Lee, K.-N. Chen, J.J.-Q. Lu, Wafer-to-Wafer Alignment for Three-Dimensional Integration: A Review, J. Microelectromech. Syst. 20 (2011) 885–898.
[12] S.H. Lee, F. Niklaus, J.J. McMahon, J. Yu, R.J. Kumar, H. Li, R.J. Gutmann, T. S. Cale, J.-Q. Lu, Fine Keyed Alignment and Bonding for Wafer-Level 3D ICs, MRS Online Proc. Libr. OPL 914 (2006).
[13] L. Shen, Ultrafast Photodetector on the InP-Membrane-on-Silicon Platform, Technische Universiteit Eindhoven, 2016.
[14] O. Shapira, Implementation of Electromagnetic Induction in Finite Rectangular Loops for Self Alignment and Levitation, 2013.
[15] S.E. Steen, D. LaTulipe, A.W. Topol, D.J. Frank, K. Belote, D. Posillico, Overlay as the key to drive wafer scale 3D integration, Microelectron. Eng. 84 (2007) 1412–1415.
[16] M. Grzesik, S.R. Vangala, W.D. Goodhue, Indirect Wafer Bonding and Epitaxial Transfer of GaSb-Based Materials, J. Electron. Mater. 42 (2013) 679–683.
[17] U. Barajas-Valdes, O.M. Suárez, Nanomechanical properties of thin films manufactured via magnetron sputtering from pure aluminum and aluminum-boron targets, Thin Solid Films 693 (2020), 137670.
[18] F. Niklaus, R.J. Kumar, J.J. McMahon, J. Yu, T. Matthias, M. Wimplinger, P. Lindner, J.Q. Lu, T.S. Cale, R.J. Gutmann, Effects of Bonding Process Parameters on Wafer-to-Wafer Alignment Accuracy in Benzocyclobutene (BCB) Dielectric Wafer Bonding, MRS Online Proc. Libr. OPL 863 (2005).
[19] N.A.M. Yahya, W.H. Lim, S.W. Phang, H. Ahmad, R. Zakaria, F.R.M. Adikan, Curing Methods Yield Multiple Refractive Index of Benzocyclobutene Polymer Film 5, 2011, p. 3.
[20] Dow Processing Procedures for CYCLOTENE 3000 Series Dry Etch Resins. http://www.dow.com/cyclotene/docs/cyclotene_3000_dry_etch.pdf, 2023. Accessed 27 July 2021.